Wet/dry status change in global closed basins between the mid-Holocene and the Last Glacial Maximum and its implication for future projection

Xinzhong Zhang[1], Yu Li[1], Wangting Ye[1], Simin Peng[1], Yuxin Zhang[1], Hebin Liu[1], Yichan Li[1], Qin Han[1], Lingmei Xu[1]

[1]Key Laboratory of Western China's Environmental Systems (Ministry of Education), College of Earth and Environmental Sciences, Center for Hydrologic Cycle and Water Resources in Arid Region, Lanzhou University, Lanzhou 730000, China

Correspondence to: Yu Li (liyu@lzu.edu.cn)

Abstract. Closed basins, mainly located in subtropic and temperate drylands, have experienced alarming declines in water storage in recent years. An assessment of long-term hydroclimate change in those regions remains unquantified at a global scale yet. By integrating lake records, PMIP3/CMIP5 simulations and modern observations, we assess the wet/dry status of global closed basins during the Last Glacial Maximum, mid-Holocene, pre-industrial, 20th and 21st century periods. Results show comparable patterns of general wetter climate during the mid-Holocene and near-future warm period, mainly attributed to the boreal summer and winter precipitation increasing, respectively. The long-term pattern of moisture change is highly related to the high-latitude ice sheets and low-latitude solar radiation, which leads to the poleward moving of westerlies and strengthening of monsoons during the interglacial period. However, modern moisture changes show correlations with El Niño/Southern Oscillation in most closed basins, such as the opposite significant correlations between North America and Southern Africa and between Central Eurasia and Australia, indicating strong connection with ocean oscillation. The strategy for combating future climate change should be more resilient to diversified hydroclimate responses in different closed basins.

1 Introduction

A great number of observations in the last 100 years show that the Earth's climate is now experiencing significant change characterized by global warming (Hansen et al., 2010; Trenberth et al., 2013; Dai et al., 2015; Huang et al., 2016; Li et al., 2018), which is unequivocally induced by the increase in concentrations of greenhouse gases according to the Fifth Assessment Report of the Intergovernmental Panel on Climate Change (IPCC, 2013). Recent studies have indicated increasing drought and accelerated dryland expansion under modern global warming resulting from a higher vapour pressure deficit and evaporative demand (Dai, 2013; Feng and Fu, 2013; Huang et al., 2017). Assessing the impacts of global warming especially on the terrestrial moisture balance is not only one of the most important social and environmental issues but also the basis of future climate projections.

According to Held's hypothesis, rising atmospheric humidity will cause the existing patterns of atmospheric moisture divergence and convergence to intensify, thereby making effective precipitation more negative in the drylands and more positive in the tropics, now referred to as the "dry gets drier, wet gets wetter" (DGDWGW) paradigm (Held & Soden, 2006; Hu et al., 2019). However, this mechanism may be more complex regionally, especially over terrestrial environments, where wet/dry pattern changes over the past decades and in future projections do not follow the proposed intensification trend (Greve et al. 2014; Roderick et al. 2014). To accurately project future terrestrial hydroclimatic changes, past climates may aid in understanding the regional nuances of the DGDWGW effect (Lowry & Morrill, 2019). Quade and Broecker (2009) have verified Held's hypothesis by taking the Last Glacial Maximum (LGM) as a reverse analog for modern global warming, and point out that the hydroclimate changes in subtropical regions are more complicated. Besides, the African Humid Period and a following mid-Holocene (MH) thermal maximum are also the focused key periods (Lézine et al., 2011), and related researches prove that gradual climate forcing can result in rapid climate responses and a remarkable transformation of the hydrologic cycle (deMenocal & Tierney, 2012). Furthermore, Burke et al. (2018) compared the six warm periods in the past including the early Eocene, mid-Pliocene, Last Interglacial, mid-Holocene, pre-Industrial (PI) and 20th century with the simulated future scenario to find the best analog for near-future climate. A long-term and large-scale evaluation on global hydroclimate change is of vital significance for a comprehensive understanding of the impact of global warming and for future climate projections.

Closed basins account for about one fifth of the global land areas and are mainly located in the arid and semi-arid climate zones. As there is no outlet or hydrological connection to the oceans, the terminal lakes function as the ocean for closed basins and concentrate the sedimentary information of the whole basin (Li et al., 2015), which makes them ideal candidates for studying the hydroclimate change of the past. Besides, they play an important role in mitigating global changes by influencing the trend and interannual variability of the terrestrial carbon sink (Ahlström et al., 2015; Li et al., 2017), though the hydrological cycle of the closed basins is fragile and sensitive to climate change. In the most recent IPCC sea level budgets, changes in terrestrial water storage driven by the climate have been assumed to be too small to be included (IPCC, 2013; Zhan et al., 2019). However, recent advances in gravity satellite measurement enabled a quantification that water storages in closed basin are declining at alarming rates, which not only exacerbate local water stress, but also impose excess water on exorheic basins, leading to a potential sea level rise that matches the contribution of nearly half of the land glacier retreat (excluding Greenland and Antarctica) (Wurtsbaugh et al., 2017; Wang et al., 2018). The influence of global warming on water availability in closed basins is far more serious than that in other regions, and understanding the pattern and mechanism of hydroclimate change in the past and modern warm periods will be the key to assess the impact of future climate change.

In this paper, we focus on the wet/dry status change between the LGM, MH and modern warm period in global closed basins to improve our knowledge of regional responses to climate change. Based on the lake records, modern observations and simulations of the key periods from the Paleoclimate Modeling Intercomparison Project Phase 3 (PMIP3) and Coupled Model Intercomparison Project Phase 5 (CMIP5), an assessment of hydroclimate change at different timescales from the LGM to MH and from the PI to late 21st century is conducted. The possible linkages of these moisture change patterns and their underlying

physical mechanisms are also discussed. This assessment is essential for future climate projection and regional water management, especially in the dry hinterland.

2 Data and methods

2.1 Water level and moisture change inferred from lake records

The following criteria were used for the selection of the proxy records in this study (Chen et al., 2015): (1) The proxies should be indicative of moisture changes. (2) The records should cover both the LGM and MH time slices. (3) The dominant driving mechanism of the variation in proxy records should be climatic changes. (4) The records should have a dating control level of 6 or better for 21 ka and 6 ka time slices according to the Cooperative Holocene Mapping (COHMAP) project dating scheme. A dating control level of 6 for continuous sequences was based on the following criteria: Bracketting dates, one within 6000 years and the other within 8000 years or one within 4000 years and the other within 10000 years of the selected date (21 ka and 6 ka). The same control level applied to discontinuous sequences requires at least one date within 2000 years of the time being assessed (Street-Perrott et al., 1989; COHMAP Members, 1994; Lowry & Morrill, 2019).

We then compared our new compilation of proxy records (Supplement Table S1) to 50 water level records from the Global Lake Status Data Base (Street-Perrott et al., 1989; COHMAP Members, 1994; Kohfeld and Harrison, 2000; Harrison et al., 2003) and Chinese lake-status database (Yu et al., 2001; Xue et al., 2017) in global closed basins and surrounding areas (Fig. 1). To capture the general spatial pattern, the differences of lake status between the LGM and MH in individual records were classified into 3 grades (higher/wetter, moderate, lower/drier). Similarly, the differences of simulated effective precipitation between the LGM and MH from PMIP3/CMIP5 multi-models in certain grid of the lake site were classified into positive, no change and negative and compared with the records.

2.2 Modern data sources and analyses

Closed basin extents were acquired from HydroBASINS product, a series of polygon layers that depict watershed boundaries and sub-basin delineations at a global scale by using the HydroSHEDS (Hydrological data and maps based on SHuttle Elevation Derivatives at multiple Scales) database at 15 arc-second resolution (Lehner et al., 2013). There were some exceptions we did not take them into account in this study: (1) Ten landlocked watersheds in the Inner Tibetan Plateau, Northeast China, Siberia and western United States were captured only in Global Drainage Basin Database (Masutomi et al., 2009; Wang et al., 2018); (2) Sporadic landlocked watersheds smaller than 100 km^2 Embedded in the exorheic regions were not considered as independent units; (3) Some of the contemporary endorheic watersheds were exorheic in the past, such as the Wuyuer river basin in Northeast China.

Primary variables of mean precipitation (P) and potential evapotranspiration (PET) from Climatic Research Unit Time-Series version 4.01(CRU TS4.01), a gridded time-series dataset of month-by-month variation in climate covering all land areas (excluding Antarctica) at 0.5° resolution over the period 1901-2016 (Harris et al., 2014), were used for modern climate analysis.

Aridity index (AI) defined as the ratio of annual precipitation to annual potential evapotranspiration by the United Nations

95 Environment Programme (UNEP, 1992) was applied. Furthermore, to explore the possible relationship between the ocean and closed basins in modern times, we carried out the pearson correlation analysis between monthly AI and multivariate El Niño/Southern Oscillation (ENSO) index (MEI) (Kobayashi et al., 2015) and other indexes such as the North Atlantic Oscillation (NAO), Southern Oscillation Index (SOI), Pacific Decadal Oscillation (PDO) and Tripole Index for the Interdecadal Pacific Oscillation (TPI) (Supplement Table S2) for different endorheic regions. Linear trend of AI change in

100 global closed basins during 1979-2016 was provided, and a trend was considered statistically significant at a significance level of 5%.

2.3 Debiasing and downscaling of PMIP3/CMIP5 multi-model ensemble

Experiments of the LGM, MH and PI from the PMIP3 and projection experiment of 21st century under Representative Concentration Pathway 8.5 (RCP8.5) from the CMIP5 were used in this study (Braconnot et al., 2012; Taylor et al., 2012). To

105 ensure the consistency and precision of simulations as much as possible, we used the outputs from 5 global climate models (Table 1) which have all completed the above key period experiments at a spatial resolution of less than 3 degrees. The periods of 2006-2015 and 2091-2100 were defined as the representatives of early and late 21 century (E21 and L21), respectively.

Statistical downscaling and debiasing followed a multi-step approach described by Tabor and Williams (2010). The primary climate variables were first debiased by differencing each paleoclimate (LGM, MH, PI) or future climate (2017-2100)

110 simulation from a present climate simulation (2006-2015). These anomalies are then downscaled through spline interpolation to a 0.5° resolution grid corresponding to the modern observational CRU dataset. The anomalies are then added to the observational data (2006-2015) to produce the debiased and downscaled primary variables for the paleoclimate or future climate simulation. This differencing removes any systematic difference as long as that bias is constant through time (Wilby et al,. 2004; Lorenz et al., 2016). The effective precipitation calculated by precipitation minus evaporation was introduced to

115 compare with the lake status during the LGM and MH, and predict future changes in moisture balance.

Table 1. PMIP3/CMIP5 models used in this study.

Model name	Resolutions	Modelling centre	References
CCSM4	288×192	National Center for Atmospheric Research, USA	(Gent et al., 2011)
CNRM-CM5	256×128	Centre National de Recherches Meteorologiques, France	(Voldoire et al., 2013)
GISS-E2-R	144×90	NASA Goddard Institute for Space Studies, USA	(Schmidt et al., 2014)
MIROC-ESM	128×64	Japan Agency for Marine-Earth Science and Technology, Japan	(Watanabe et al., 2011)
MRI-CGCM3	320×160	Meteorological Research Institute, Japan	(Yukimoto et al., 2012)

3 Results

3.1 Wet/dry status changes from lake records
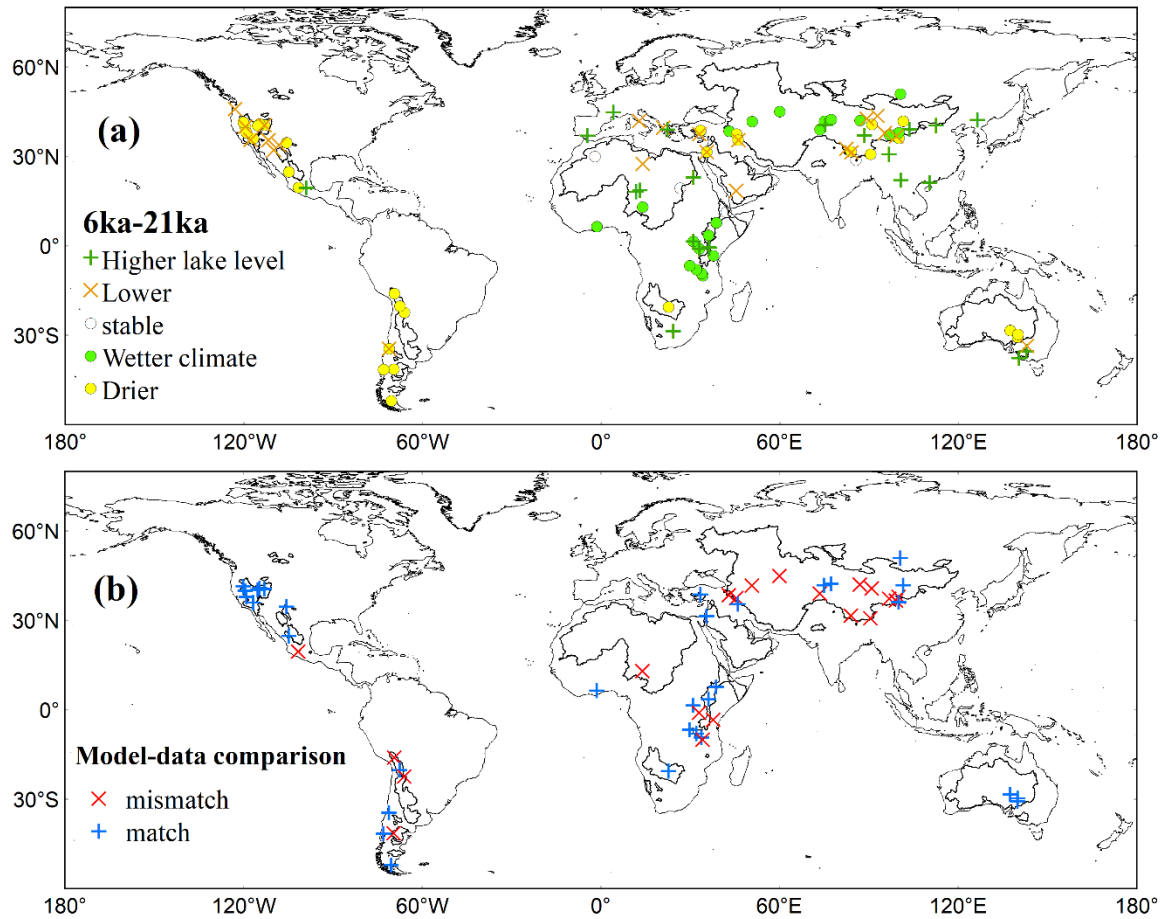
Figure 1. Wet/dry status changes between the LGM and MH from lake records (a) and comparison with the simulated effective precipitation from PMIP3/CMIP5 multi-models (b). The green and yellow cross sites are from lake status databases; the green and yellow point sites are from recently published literatures; the hollow points indicate that there is no significant change in lake level or climate condition between the LGM and MH.

Generally, lake level changes match climate changes from the proxy records well except for Central Asia (Fig. 1). In the North and South American continents, almost all closed basins experience a wetter LGM compared to the MH status, and the same situations exist in some closed basins of Eastern Mediterranean, Tibetan Plateau and Australia. On the contrary, Eastern African highlands and the Sahel region show a prevailing wetter MH, which may be highly attributed to the African Humid

130   Period. Changes in Central Eurasia are more complicated. The monsoonal Eastern Asia and arid Central Asia both record wetter MH, while in the middle area between them, there are some contradictory records synchronously showing lower lake level and wetter climate. Though evidence from Southern Africa and Australia are insufficiency, several records tend to support a wetter LGM. Hereto, it is worth noting that there are two belt regions around latitude 30 degrees at both Hemisphere where substantial high lake levels during the LGM have disappeared or subsided during the MH. And the low-latitude Africa and

135   mid-latitude Asia basically experience an opposite pattern of a wetter MH.

    Comparison between the wet/dry status change from new compilation of proxy records and simulated effective precipitation from PMIP3/CMIP5 multi-models is shown in Fig. 1b. The model ensemble does particularly well in simulating the direction of hydroclimate change in most closed basins of Americas, Africa and Australia. The most mismatches exist in the Central Eurasia, since many lake records suggest wetter climate during MH whereas the model ensemble does not. Some minor

140   mismatches occur in the East Africa and South America, where the altitude changes dramatically so that the models may appear to miss the details of climate change.

3.2 Simulated climate changes under the past and future warming
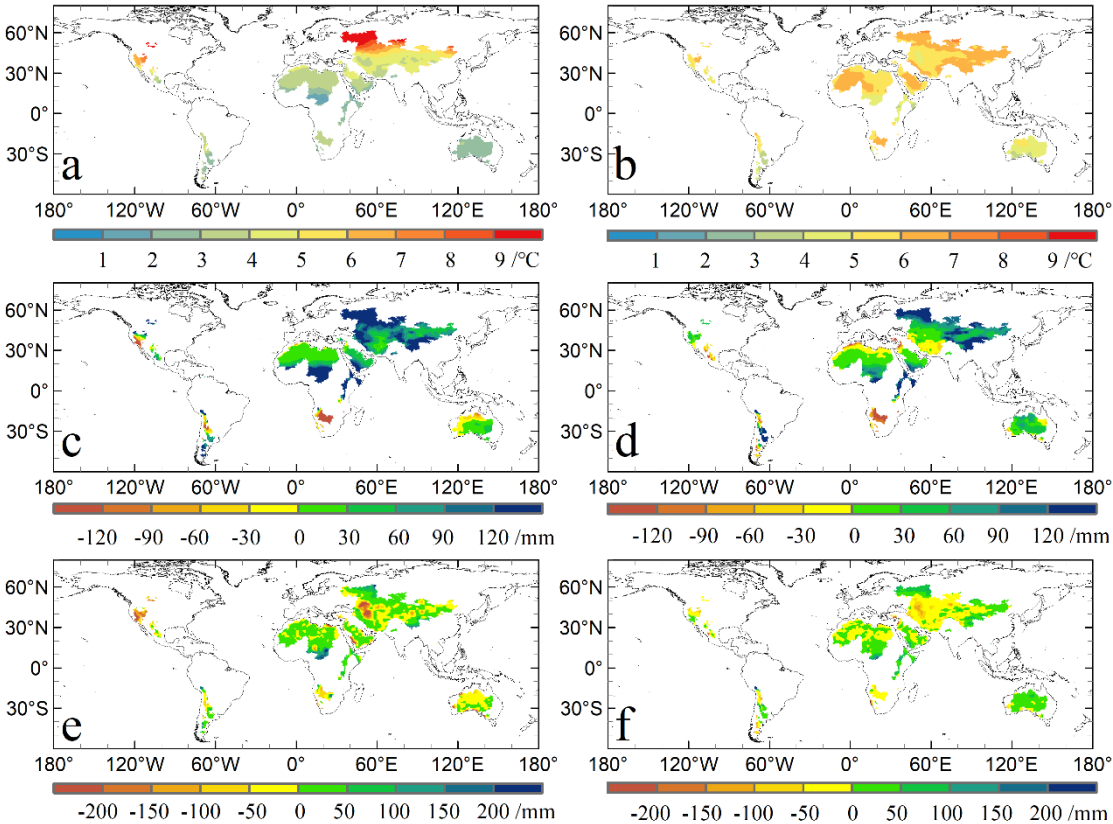
Figure 2. Annual mean temperature (a,b), precipitation (c,d) and effective precipitation (e,f) differences for MH-LGM (left) and L21-PI (right) in global closed basins based on the PMIP3/CMIP5 multi-model ensemble.

Spatial patterns of hydroclimate change for MH-LGM and L21-PI are shown in Fig. 2. It's apparent that the MH warming is characterized by strong latitudinal zonality, while future warming is more homogeneous over all closed basins.The temperature rise by the end of this century will exceed that during the period of LGM-MH in most closed basins under RCP8.5 scenario (excluding the high latitudes of North America and Central Asia). On the contrary, precipitation increasing under future warming is lighter and keep the similar distribution pattern of MH. The dramatic shifts of precipitation change bettwen the two periods exist in the subtropics such as the dry-wet shifts in the Mediterranean coast, Mexican Plateau and Iranian Plateau. For the pattern of effective precipitation change, it's substantially fragmented. The prevailing wetter climate in North Africa and Central Eurasia during the MH is weakened while Australia gets wetter in the future. As a consequence, the core area of drought is moved from Western America during the MH to Central Asia by the end of this century.

Table 2. Percentage changes of monthly precipitation and evaporation between different periods from the multi-models.

		Jan.	Feb.	Mar.	Apr.	May	Jun.	Jul.	Aug.	Sep.	Oct.	Nov.	Dec.
MH-LGM	P	8.3	2.0	-1.1	9.7	25.8	32.1	41.1	52.7	57.5	46.0	34.8	18.1
	E	17.1	11.0	10.9	16.0	27.4	36.1	40.2	43.7	42.4	35.9	30.7	24.9
L21-PI	P	10.8	12.1	12.6	14.4	8.3	-1.5	1.5	6.5	8.3	11.3	11.6	11.4
	E	9.5	10.2	11.6	14.5	12.8	9.5	6.5	7.9	6.8	4.9	6.5	9.5
L21-E21	P	9.3	7.7	8.9	12.7	7.3	-1.0	4.6	8.2	6.2	8.0	6.5	7.9
	E	8.4	7.9	8.3	12.0	10.7	8.8	6.7	8.4	6.7	5.4	4.6	7.1

To investigate the seasonal difference of hydroclimate change, we assess the percentage changes of monthly precipitation and evaporation during the MH, modern and future warm periods at a global scale (Table 2). It turns out that remarkable increases of precipitation and evaporation mainly occur in the boreal summer half-year during the MH, while in modern and future warm periods they are concentrated in the boreal winter half-year. The precipitation increases about 50% from the LGM to the MH in the wettest months of July-October, 13% from PI to L21 in the wettest months of February-April. Seasonal variation in evaporation is smaller than that in precipitation but keep the same pattern. In addition, precipitation and evaporation changes from E21 to L21 make significant contributions to the increasing of precipitation and evaporation from PI to L21, especially in the boreal summer half-year.

3.3 Moisture trends and connections of modern observations
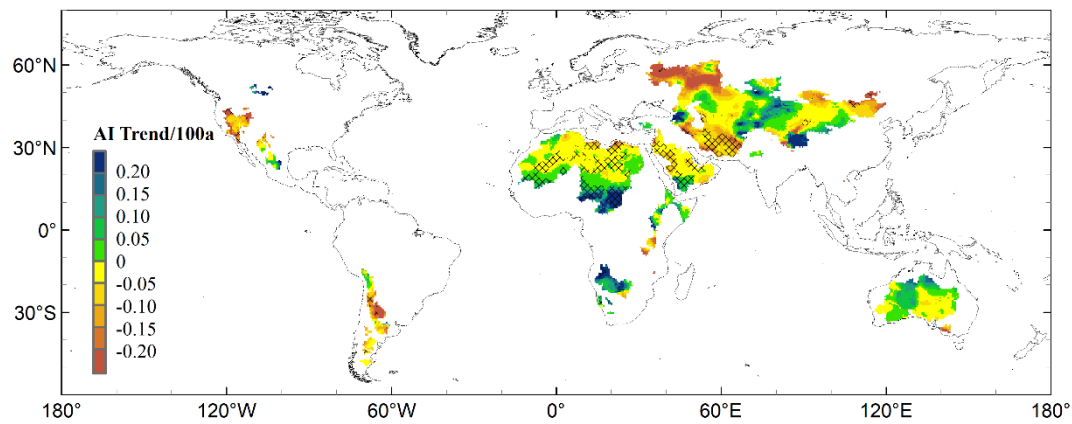
Figure 3. Linear trends of modern observational AI for the period of 1979-2016 in global closed basins. Gridding areas are where the trends are statistically significant at 5% level.

Over the past four decades, as shown in Fig. 3, about 70% of the total areas of global closed basins are getting drier. The severe drying regions include the Great Basin and the Patagonia in Americas and the Upper Volga river basin and Iran Plateau in Central Eurasia. The wetting trends mainly occur in the low latitudes of Africa and the high altitudes of Asia including the Caucasus Mountains, the Tianshan Mountains, the Pamir and Tibetan Plateau. Besides, the marginal closed basins of East Asia and North Australia as well as the Mexican Plateau and the Altiplano in the Americas show lighter wetting trends. It's worth noting that the future pattern of effective precipitation change (Fig. 2f) mainly continues the trends of modern moisture change, with the most significant mismatch in Southern Africa. That means the mechanism of future hydroclimate change likely keep the same as modern times in most closed basins.

Table 3. Pearson correlation coefficients between annual AI and monthly MEI during 1979-2016. The bold numbers mean that correlation coefficients are statistically significant at 5% level. SAM-South America, NAM-North America, SAF-Southern Africa, EAF-Eastern Africa, NAF-Northern Africa and Arabian peninsula, CEA-Central Eurasia, AUS-Australia, ALL-global closed basins.

	Jan.	Feb.	Mar.	Apr.	May	Jun.	Jul.	Aug.	Sep.	Oct.	Nov.	Dec.
SAM	-0.23	-0.26	-0.15	-0.05	-0.05	0.08	0.22	0.29	0.27	0.22	0.14	0.19
NAM	**0.47**	**0.52**	**0.55**	**0.50**	**0.47**	0.30	0.06	-0.02	0.01	-0.01	-0.01	-0.02
SAF	**-0.60**	**-0.57**	**-0.60**	**-0.64**	**-0.53**	**-0.37**	-0.15	0.01	-0.07	-0.10	0.00	0.00
EAF	-0.02	-0.06	-0.12	-0.07	0.01	-0.01	-0.02	0.08	0.10	0.16	0.25	0.28
NAF	0.03	0.01	-0.03	-0.09	-0.09	-0.05	0.00	0.01	0.05	0.10	0.14	0.11

CEA	0.19	0.16	0.13	0.19	0.31	**0.45**	**0.50**	**0.47**	**0.47**	**0.45**	**0.43**	**0.41**
AUS	0.06	0.09	0.09	0.13	0.06	-0.13	-0.28	-0.28	**-0.32**	**-0.34**	**-0.37**	**-0.36**
ALL	-0.02	-0.05	-0.09	0.02	0.13	0.24	0.30	**0.38**	**0.36**	**0.37**	**0.41**	**0.42**

185

By calculating the pearson correlation coefficients between annual AI and monthly MEI, NAO, SOI, PDO and TPI, we seek for the potential connections of moisture change in closed basins with ocean oscillation. As results, the performance of NAO, SOI and PDO are comparatively weak, and the MEI responds the best and shows the similar pattern as TPI does, both indicating the dominant role of the Pacific Ocean oscillation in controlling the moisture change of global closed basins (Table 3, Supplement Table S2). For the global closed basins as a whole, the AI change is significantly positive related to monthly MEI from August to December, and the correlation coefficient reaches its highest in December of boreal winter season. As the biggest part of global closed basins, Central Eurasia apparently contributed the most in this positive feedback. On the contrary, in the Australian closed basins it's lightly negative correlated with monthly MEI during almost the same seasons. Among the seven separated endorheic regions, AI changes in South America, Eastern and Northern Africa show no significant correlation with MEI at all. For the other four regions, they are seemingly coupled between North America and Southern Africa and between Central Eurasia and Australia with the opposite significant AI-MEI relationships. During the first half year, North America responds positively whereas Southern Africa shows negative response to the MEI change. The same pattern turns to Central Eurasia and Australia in the second half year. This provides a potential perspective on the teleconnections in different closed basins globally.

4 Discussion

Closed basins are mainly located in subtropic and temperate drylands, where the hydroclimate changes deeply depend on the limited moisture transport via atmospheric circulation. Based on this, among the seven separated endorheic regions mentioned before, most of them can be divided into two parts: the westerlies-dominated area and the monsoon-influenced area, such as Central Asia and East Asia in Central Eurasia as well as the Western United States and the Mexican Plateau in North America. Thus, their climate changes are strongly influenced by the interactions of mid-latitude westerlies and low-latitude monsoon especially on a long-term timescale (Li et al., 2013; Li et al., 2017; Chen et al., 2019; Li et al., 2020). On a shorter timescale of modern times, internal variability of climate system like the ocean oscillations rather than the external forcing plays more important roles in controlling the regional moisture change (Wang et al., 2018). Though the driving mechanism may be extensively changed, our results show that hydroclimate changes in some closed basins respond in the same pattern to the past and future warming, indicating deeper connections at different timescales. More importantly, the long-term hydroclimate change patterns provide the baseline for modern and future climate change assessment (IPCC, 2013).
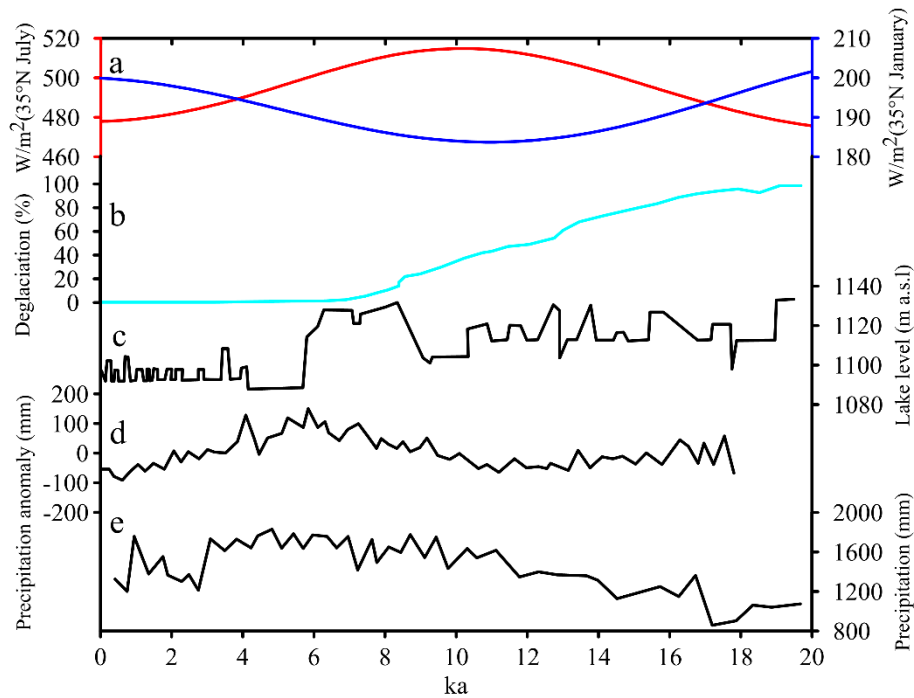
Figure 4. Changes of insolation, ice sheet and typical lake records since the LGM. (a) Summer and winter insolation variations at 35°N (Laskar et al., 2004); (b) Percent area change of ice sheets in North America (Dyke, 2004); (c) Lake-level variation from Owens Lake, Western USA (Bacon et al., 2020); (d) Pollen-based annual mean precipitation record for Lakes Dalianhai and Qinghai on the northeastern Qinghai-Tibet Plateau, Western China (Li et al., 2017); (e) Pollen-based annual precipitation change (modern analogues technique) at Lake Barombi Mbo, Northern Africa (Lebamba et al., 2012).

Previous studies have indicated that the hydroclimate change patterns in different latitudes at the millennial, centurial and decadal timescales show considerable connection with the general atmospheric circulation, which is mainly forced by the external forcing at a long-term timescale and by the internal factors of climate system at a shorter timescale (Kohfeld et al., 2013; Tierney et al., 2013; Ljungqvist et al., 2016; Zhang et al., 2017). From the perspective of paleoclimatology, the MH was extremely different from the LGM in the strengths and positions of monsoons and westerlies induced by the primary drivers such as solar insolation, Arctic warming and continental ice sheets (Sime et al., 2016; Wang et al., 2017; Bhattacharya et al., 2018; Routson et al., 2019; Jansen et al., 2020). Besides, it was also considered that the increase of atmospheric CO_2 concentration and early human activities are important driving forces for the changes of climate and lake level since the LGM (Shakun et al., 2010; Li et al., 2013; Miebach et al., 2016; Jenny et al., 2019). From the LGM to the early Holocene, it was characterized with retreat of continental ice sheets and increasing of summer insolation in the North Hemisphere (Fig. 4). During the LGM, the westerlies in the Northern Hemisphere moved south reaching the southwest of the United States, the eastern Mediterranean region and southern Tibetan Plateau, because of the development of continental ice sheets in the North

Hemisphere such as the Laurentian Ice Sheet in North America (Claire et al., 2010; Lachniet et al., 2014; Lowry & Morrill, 2019; Batchelor et al., 2019). Also, the high winter insolation enhanced evaporation and moisture transport, resulting in higher winter precipitation compared to the MH. Thus, many lakes in westerlies North America such as Owens Lake maintain high lake level during the whole deglaciation period (Fig. 4c). On the contrary, summer insolation in the North Hemisphere reached

235 its highest status during the early Holocene, leading to strengthening and expansion of monsoon by amplifying regional sea-land thermal contrast (An et al., 2000; Li & Harrison, 2008; Wang et al., 2017).

Evidences from paleoclimatic records and simulations in Northern Africa had shown that the world's largest desert in modern times experienced a humid period and was covered by forests and lakes due to the strengthening of the African monsoon during the early and middle Holocene (Lézine et al., 2011; Lebamba et al., 2012; Contoux et al., 2013; Hély et al.,

240 2014; Shanahan et al., 2015). And this kind of shifts were recorded in many monsoonal regions globally, including closed basins in Americas, Asia and Australia (Magee et al., 2004; Zhang et al., 2011; Kuhnt et al., 2015; Metcalfe et al., 2015; Bernal et al., 2016). As the most typical monsoon system, Asian summer monsoon even reached as far as the Tianshan Mountains and Kunlun Mountains of Central Asia during the Holocene (Wang et al., 2014; Ramisch et al., 2016), bringing monsoon precipitation and reforming the hydroclimate pattern in the eastern closed basins of Central Eurasia. Even in modern times,

245 the monsoon moisture could invade western Qilian Mountains and impact on precipitation especially the heavy precipitation events (Du et al., 2020). However, from the LGM to MH, hydroclimate changes in Central Euraisa were more complicated than that in other regions, due to the strong interactions of westerlies and monsoon in the middle region between the arid Central Asia and monsoonal Eastern Asia. As a consequence of moving of westerlies, the effective precipitation in arid Central Asia didn't increase until the middle and late Holocene, leading to a large number of low lake levels and showing different

250 climate response pattern compared with that in monsoonal Eastern Asia corresponding to the summer insolation change (Chen et al., 2008; Ran et al., 2013; Huang et al., 2014; Chen et al., 2019).

The difference in moisture change between the arid Central Asia and monsoonal Asia still exists in modern times and near-future warm period, and it is more apparent between the high altitudes and lower basins from the modern observations (Fig. 3). On a shorter timescale of modern times, strengthening or moving of monsoons and westerlies are largely limited compared

255 to that from the LGM to MH. As results shown before, ocean oscillation especially the Pacific Ocean oscillation emphasize its impact on controlling the moisture change of global closed basins, with two couples of the opposite significant AI-MEI relationships between the North America and the Southern Africa and between the Central Eurasia and the Australia (Table 3). The ENSO-based composite analyses have shown that the water vapor fluxes of seasonal precipitation in Central Eurasia are mainly generated in Indian and North Atlantic Oceans and transported by enhanced westerlies during EI Nino events

260 (Mariotti, 2007; Rana et al., 2017; Xi et al., 2018; Rana et al., 2019). Based on the simulation of future climate change, evidence shows that the winter precipitation play a dominant role in determining the wet/dry pattern change in global closed basins, implying the significance of westerlies instead of monsoon. These patterns provide some new perspectives to understand the differences and connections over global closed basins and remind us that we should focus more on the ocean oscillations in order to address the challenges of future climate change.

5 Conclusion

This study presents a new compilation of lake records and analyses of hydroclimate change at different timescales in global closed basins. Though it's well known that the forcing mechanisms between mid-Holocene and future warming are different, the patterns of hydroclimate changes of them show comparable spatial consistency in closed basins. From the LGM to the MH, the westerlies-dominated areas usually experience wet to dry shift whereas the monsoon-influenced areas shift from drier to wetter climate. The hydroclimate changes from the PI to the Late 21st century show the similar patterns in most closed basins, except for Central Asia where it is wetter during the MH but drier during the future warm period. For the global closed basins as a whole, it's wetter both in the MH and L21 than that during the LGM and PI. However, they are mainly attributed to the boreal summer and winter precipitation increasing, respectively. The seasonal difference of precipitation increasing indicates the different dominant roles of westerly winds and monsoons during the two periods. That is, the long-term regional differences of hydroclimate change are mainly controlled by the high-latitude ice sheets and low-latitude solar radiation, which leads to equatorward moving of the westerlies during the glacial period and the strengthening of monsoons during the interglacial period. An analynis of modern moisture change matching with the timescale of future warming suggests that it's related to ocean oscillations especially the Pacific Ocean oscillation, such as the two coupled opposite significant AI-MEI relationships between the North America and the Southern Africa and between the Central Eurasia and the Australia. Though the dryland expansion may be accelerated under the near future warming in the hinterland globally, we can't ignore the hydroclimate response differences within these regions, which largely affect the local strategies of economic development and environmental protection. We must be more resilient to tackle the future climate change corresponding to diversified hydroclimate changes in different closed basins.

Data Availability. Boundaries of closed basins are available from the Hydrological data and maps based on SHuttle Elevation Derivatives at multiple Scales (HydroSHEDS) website https://www.hydrosheds.org/page/hydrobasins. The Global Lake Status Data Base and Chinese lake-status database are available from the Paleoclimatology Datasets of NOAA's National Centers for Environmental Information (NCEI) https://www.ncdc.noaa.gov/data-access/paleoclimatology-data/datasets. PMIP3/CMIP5 simulations are available from the Earth System Grid Federation (ESGF) Peer-to-Peer (P2P) enterprise system website https://esgf-node.llnl.gov/projects/esgf-llnl/. CRU TS4.01 data are available from https://crudata.uea.ac.uk/cru/data/hrg/. The Values of MEI, NAO, SOI, PDO and TPI are available from https://psl.noaa.gov/data/climateindices/list/. Details about the new compilation of proxy records are available in Supplement.

Author contributions. Yu Li and Xinzhong Zhang designed this study and carried it out. Wangting Ye, Yuxin Zhang and Simin Peng contributed to the data processing, analysis and discussion of results. Xinzhong Zhang prepared the manuscript with contributions from all co-authors.

Competing interests. The authors declare that they have no conflict of interest.

Acknowledgements. This work was supported by the National Natural Science Foundation of China (Grant Nos. 41822708 and 41571178), the Strategic Priority Research Program of Chinese Academy of Sciences (Grant No. XDA20100102), the Fundamental Research Funds for the Central Universities (Grant No. lzujbky-2018-k15) , and the Second Tibetan Plateau Scientific Expedition (STEP) program (Grant No. XDA20060700).

References

Ahlström, A., Raupach, M. R., Schurgers, G., Smith, B., Arneth, A., Jung, M., Reichstein, M., Canadell, J. G., Friedlingstein, P., Jain, A. K., Kato, E., Poulter, B., Sitch, S., Stocker, B. D., Viovy, N., Wang, Y., Wiltshire, A., Zaehle, S., & Zeng, N. (2015). The dominant role of semi-arid ecosystems in the trend and variability of the land CO_2 sink. Science, 348(6237), 895-899.

An, Z., Porter, S. C., Kutzbach, J. E., Wu, X., Wang, S., Liu, X., Li, X., & Zhou, W. (2000). Asynchronous Holocene optimum of the East Asian monsoon. Quaternary Science Reviews, 19(8), 743-762.

Bacon, S., Jayko, A., Owen, L., Lindvall, S., Rhodes, E., Schumer, R., & Decker, D. (2020). A 50,000-year record of lake-level variations and overflow from Owens Lake, eastern California, USA. Quaternary Science Reviews, 238, 106312.

Batchelor, C. L., Margold, M., Krapp, M., Murton, D. K., Dalton, A. S., Gibbard, P. L., Stokes, C. R., Murton, J. B., & Manica, A. (2019). The configuration of Northern Hemisphere ice sheets through the Quaternary. Nature communications, 10(1), 1-10.

Bernal, J. P., Cruz, F. W., Stríkis, N. M., Wang, X., Deininger, M., Catunda, M. C. A., Ortega-Obregóna, C., Cheng, H., Edwards, R. L., & Auler, A. S. (2016). High-resolution Holocene South American monsoon history recorded by a speleothem from Botuverá Cave, Brazil. Earth and Planetary Science Letters, 450, 186-196.

Bhattacharya, T., Tierney, J. E., Addison, J. A. & Murray, J. W. (2018) Ice-sheet modulation of deglacial North American monsoon intensification, Nature Geoscience, 11(11), 848–852.

Braconnot, P., Harrison, S. P., Kageyama, M., Bartlein, P. J., Masson-Delmotte, V., Abe-Ouchi, A., & Zhao, Y. (2012). Evaluation of climate models using palaeoclimatic data. Nature Climate Change, 2(6), 417.

Burke, K. D., Williams, J. W., Chandler, M. A., Haywood, A. M., Lunt, D. J., & Otto-Bliesner, B. L. (2018). Pliocene and Eocene provide best analogs for near-future climates. Proceedings of the National Academy of Sciences, 115(52), 13288-13293.

Chen, F., Yu, Z., Yang, M., Ito, E., Wang, S., Madsen, D. B., & Boomer, I. (2008). Holocene moisture evolution in arid central Asia and its out-of-phase relationship with Asian monsoon history. Quaternary Science Reviews, 27(3-4), 351-364.

Chen, F., Chen, J., Huang, W., Chen, S., Huang, X., Jin, L., Jia, J., Zhang, X., An, C., Zhang, J., Zhao, Y., Yu, Z., Zhang, R., Liu, J., Zhou, A., & Feng, S. (2019). Westerlies Asia and monsoonal Asia: Spatiotemporal differences in climate change and possible mechanisms on decadal to sub-orbital timescales. Earth-Science Reviews, 192, 337-354.

Chen, J., Chen, F., Feng, S., Huang, W., Liu, J., & Zhou, A. (2015). Hydroclimatic changes in China and surroundings during the Medieval Climate Anomaly and Little Ice Age: spatial patterns and possible mechanisms. Quaternary Science Reviews, 107, 98-111.

Claire, M. C., & Rambeau. (2010). Palaeoenvironmental reconstruction in the southern levant: synthesis, challenges, recent developments and perspectives. Philosophical Transactions of the Royal Society A: Mathematical, Physical and Engineering Sciences, 368, 5225-5248.

COHMAP Members. (1994). Oxford Lake Levels Database. IGBP PAGES/World Data Center- A for Paleoclimatology Data Contribution Series # 94-028. NOAA/NGDC Paleoclimatology Program, Boulder CO, USA.

Contoux, C., Jost, A., Ramstein, G., Sepulchre, P., Krinner, G., & Schuster, M. (2013). Megalake Chad impact on climate and vegetation during the late Pliocene and the mid-Holocene. Climate of the Past, 9, 1417-1430.

Cook, K. H. (2000). A southern hemisphere wave response to enso with implications for southern africa precipitation. Journal of Atmospheric Sciences, 58(15), 2146-2162.

Dai, A. (2013). Increasing drought under global warming in observations and models. Nature Climate Change, 3(1), 52-58.

Dai, A., Fyfe, J. C., Xie, S. P., & Dai, X. (2015). Decadal modulation of global surface temperature by internal climate variability. Nature Climate Change, 5(6), 555-559.

deMenocal, P. B., & Tierney, J. E. (2012). Green Sahara: African humid periods paced by earth's orbital changes. Nature Education Knowledge, 3(10), 12.

Dyke, A. S. (2004) An outline of North American deglaciation with emphasis on central and northern Canada. Developments in Quaternary Sciences, 2, 373-424.

Feng, S., & Fu, Q. (2013). Expansion of global drylands under a warming climate. Atmospheric Chemistry and Physics, 13(10), 081-100.

Garcia, D. (2010). Robust smoothing of gridded data in one and higher dimensions with missing values. Computational statistics & data analysis, 54(4), 1167-1178.

Gent, P. R., Danabasoglu, G., Donner, L. J., Holland, M. M., Hunke, E. C., Jayne, S. R., Lawrence, D. M., Neale, R. B., Rasch, P. J., and Vertenstein, M. (2011). The community climate system model version 4. Journal of Climate, 24 (19), 4973-4991.

Greve, P., Orlowsky, B., Mueller, B., Sheffield, J., Reichstein, M., & Seneviratne, S. I. (2014). Global assessment of trends in wetting and drying over land. Nature Geoscience, 7(10), 716-721.

Hansen, J., Ruedy, R., Sato, M., & Lo, K. (2010). Global surface temperature change. Reviews of Geophysics, 48(4).

Harris, I., Jones, P.D., Osborn, T.J. & Lister, D.H. (2014), Updated high-resolution grids of monthly climatic observations – the CRU TS3.10 Dataset. International Journal of Climatology, 34, 623–642.

Held, I. M., & Soden, B. J. (2006). Robust responses of the hydrological cycle to global warming. Journal of Climate, 19(21), 5686-5699.

Hély, C., Lézine, A. M., & APD contributors. (2014). Holocene changes in African vegetation: Tradeoff between climate and water availability. Climate of the Past, 10, 681-686.

365   Holmgren, M., Stapp, P., Dickman, C. R., Gracia, C., Graham, S., & Gutiérrez, J. R., et al. (2006). A synthesis of enso effects on drylands in australia, north america and south america. Advances in Geosciences, 6(6), 69-72.

Hu, Z., Chen, X., Chen, D., Li, J., Wang, S., Zhou, Q., Yin, G., and Guo, M. (2019), "Dry gets drier, wet gets wetter": A case study over the arid regions of central Asia, International Journal of Climatology, 39(2), 1072-1091.

Huang, J., Li, Y., Fu, C., Chen, F., Fu, Q., Dai, A., & Zhang, L. (2017). Dryland climate change: Recent progress and challenges.
370   Reviews of Geophysics, 55(3), 719-778.

Huang, J., Yu, H., Guan, X., Wang, G., & Guo, R. (2016). Accelerated dryland expansion under climate change. Nature Climate Change, 6(2), 166.

Huang, X., Oberhansli, H., Von Suchodoletz, H., Prasad, S., Sorrel, P., Plessen, B., Mathis, M., & Usubaliev, R. (2014). Hydrological changes in western central asia (kyrgyzstan) during the holocene as inferred from a palaeolimnological study
375   in lake son kul. Quaternary Science Reviews, 103, 134-152.

IPCC. (2013). Climate Change 2013: The Physical Science Basis. Contribution of Working Group I to the Fifth Assessment Report of the Intergovernmental Panel on Climate Change. Cambridge University Press, Cambridge, United Kingdom.

Jansen, E., Christensen, J. H., Dokken, T., Nisancioglu, K. H., Vinther, B. M., Capron, E., Guo, C., Jensen, M. F., Langen, P. L., Pedersen, R. A., Yang, S., Bentsen, M., Kjær, H. A., Sadatzki, H., Sessford, E., & Stendel, M. (2020). Past perspectives
380   on the present era of abrupt Arctic climate change. Nature Climate Change, 10, 714-721.

Jenny, J. P., Koirala, S., Gregory-Eaves, I., Francus, P., Niemann, C., Ahrens, B., Brovkin, V., Baud, A., Ojala, A., Normandeau, A., Zolitschka, B., & Carvalhais, N. (2019). Human and climate global-scale imprint on sediment transfer during the Holocene. Proceedings of the National Academy of Sciences, 116(46), 22972-22976.

Kobayashi, S., Ota, Y., Harada, Y., Ebita, A., Moriya, M., Onoda, H., Onogi, K., Kamahori, H., Kobayashi, C., Endo, H.,
385   Miyaoka, K., & Takahashi, K. (2015). The JRA-55 Reanalysis: general specifications and basic characteristics. Journal of the Meteorological Society of Japan. 93, 5-48.

Kohfeld, K. E., Graham, R. M., Boer, A. M. D., Sime, L. C., Wolff, E. W., Quéré, C. L., & Boop, L. (2013). Southern hemisphere westerly wind changes during the last glacial maximum: paleo-data synthesis. Quaternary Science Reviews, 68(15), 76-95.

390   Kuhnt, W., Holbourn, A., Xu, J., Opdyke, B., De Deckker, P., Röhl, U., & Mudelsee, M. (2015). Southern Hemisphere control on Australian monsoon variability during the late deglaciation and Holocene. Nature communications, 6(1), 1-7.

Lachniet, M. S., Denniston, R. F., Asmerom, Y., & Polyak, V. J. (2014). Orbital control of western north america atmospheric circulation and climate over two glacial cycles. Nature Communications, 5:3805.

Laskar, J., Robutel, P., Joutel, F., Gastineau, M., Correia, A.C.M., & Levrard, B. (2004). A long term numerical solution for the insolation quantities of the Earth. Astronomy and Astrophysics, 428, 261-285.

Lebamba, J., Vincens, A., & Maley, J. (2012). Pollen, vegetation change and climate at Lake Barombi Mbo (Cameroon) during the last ca. 33 000 cal yr BP: a numerical approach. Climate of the Past, 8(1), 59-78.

Lehner, B., & Grill G. (2013). Global river hydrography and network routing: baseline data and new approaches to study the world's large river systems. Hydrological Processes, 27(15), 2171–2186.

Lézine, A. M., Hély, C., Grenier, C., Braconnot, P., & Krinner, G. (2011). Sahara and Sahel vulnerability to climate changes, lessons from Holocene hydrological data. Quaternary Science Reviews, 30(21-22), 3001-3012.

Li, G., Zhang, H., Liu, X., Yang, H., Wang, X., Zhang, X., Jonell, T., Zhang, Y., Huang, X., Wang, Z., Wang, Y., Yu, L., & Xia, D. (2020). Paleoclimatic changes and modulation of East Asian summer monsoon by high-latitude forcing over the last 130,000 years as revealed by independently dated loess-paleosol sequences on the NE Tibetan Plateau. Quaternary Science Reviews, 237, 106283.

Li, J., Dodson, J., Yan, H., Cheng, B., Zhang, X., Xu, Q., Ni, J., & Lu, F. (2017). Quantitative precipitation estimates for the northeastern Qinghai-Tibetan Plateau over the last 18,000 years. Journal of Geophysical Research: Atmospheres, 122(10), 5132-5143.

Li, X., Liu, X., Qiu, L., An, Z., & Yin, Z. Y. (2013). Transient simulation of orbital-scale precipitation variation in monsoonal East Asia and arid central Asia during the last 150 ka. Journal of Geophysical Research: Atmospheres, 118(14), 7481-7488.

Li, Y., & Harrison, S. P. (2008). Simulations of the impact of orbital forcing and ocean on the Asian summer monsoon during the Holocene. Global and Planetary Change, 60(3-4), 505-522.

Li, Y., & Morrill, C. (2013). Lake levels in Asia at the Last Glacial Maximum as indicators of hydrologic sensitivity to greenhouse gas concentrations. Quaternary Science Reviews, 60, 1-12.

Li, Y., Liu, Y., Ye, W., Xu, L., Zhu, G., Zhang, X., & Zhang, C. (2018). A new assessment of modern climate change, China— An approach based on paleo-climate. Earth-Science Reviews, 177, 458-477.

Li, Y., Wang, Y. G., Houghton, R. A., & Tang, L. S. (2015). Hidden carbon sink beneath desert. Geophysical Research Letters, 42(14), 5880-5887.

Li, Y., Zhang, C., Wang, N., Han, Q., Zhang, X., Liu, Y., Xu, L., & Ye, W. (2017). Substantial inorganic carbon sink in closed drainage basins globally. Nature Geoscience, 10(7), 501-506.

Ljungqvist, F. C., Krusic, P. J., Sundqvist, H. S., Zorita, E., Brattstr, M, G., & Frank, D. (2016). Northern hemisphere hydroclimate variability over the past twelve centuries. Nature, 532(7597), 94-98.

Lorenz, D. J., Nieto-Lugilde, D., Blois, J. L., Fitzpatrick, M. C., & Williams, J. W. (2016). Downscaled and debiased climate simulations for North America from 21,000 years ago to 2100AD. Scientific data, 3, 160048.

Lowry, D. P., & Morrill, C. (2019). Is the Last Glacial Maximum a reverse analog for future hydroclimate changes in the Americas?. Climate Dynamics, 52(7-8), 4407-4427.

Magee, J. W., Miller, G. H., Spooner, N. A., & Questiaux, D. (2004). Continuous 150 ky monsoon record from Lake Eyre, Australia: insolation-forcing implications and unexpected Holocene failure. Geology, 32(10), 885-888.

Mariotti, A. (2007). How ENSO impacts precipitation in southwest central Asia. Geophysical Research Letters, 34(16), L16706.

Masutomi, Y., Inui, Y., Takahashi, K. & Matsuoka, Y. (2009). Development of highly accurate global polygonal drainage basin data. Hydrological Processes, 23, 572–584.

Metcalfe, S. E., Barron, J. A., & Davies, S. J. (2015). The Holocene history of the North American Monsoon:'known knowns' and 'known unknowns' in understanding its spatial and temporal complexity. Quaternary Science Reviews, 120, 1-27.

Miebach, A., Niestrath, P., Roeser, P., & Litt, T. (2016). Impacts of climate and humans on the vegetation in northwestern Turkey: palynological insights from Lake Iznik since the Last Glacial. Climate of the Past, 12(2), 575-593.

Quade, J., & Broecker, W. S. (2009). Dryland hydrology in a warmer world: Lessons from the Last Glacial period. The European Physical Journal Special Topics, 176(1), 21-36.

Ramisch, A., Lockot, G., Haberzettl, T., Hartmann, K., Kuhn, G., Lehmkuhl, F., Schimpf, S., Schulte, P., Stauch, G., Wang, R., Wünnemann, B., Yan, D., Zhang, Y. & Diekmann, B. (2016). A persistent northern boundary of Indian Summer Monsoon precipitation over Central Asia during the Holocene, Scientific Reports, 6(1), 1-7.

Ran, M., & Feng, Z. (2013). Holocene moisture variations across china and driving mechanisms: a synthesis of climatic records. Quaternary International, 313-314, 179-193.

Rana, S., Mcgregor, J., & Renwick, J. (2017). Wintertime precipitation climatology and enso sensitivity over central southwest asia. International Journal of Climatology, 37(3).

Rana, S., McGregor, J., & Renwick, J. (2019). Dominant modes of winter precipitation variability over Central Southwest Asia and inter-decadal change in the ENSO teleconnection. Climate Dynamics, 53(9-10), 5689-5707.

Roderick, M., Sun, F., Lim, W. H., & Farquhar, G. (2014). A general framework for understanding the response of the water cycle to global warming over land and ocean. Hydrology and Earth System Sciences, 18, 1575–1589.

Routson, C. C., McKay, N. P., Kaufman, D. S., Erb, M. P., Goosse, H., Shuman, B. N., Rodysill, J. R. & Ault, T. (2019). Mid-latitude net precipitation decreased with Arctic warming during the Holocene, Nature, 568(7750), 83–87

Schmidt, G. A., Kelley, M., Nazarenko, L., Ruedy, R., Russell, G. L., Aleinov, I., Bauer, M., Bauer, S. E., Bhat, M. K., & Bleck, R. (2014). Configuration and assessment of the GISS ModelE2 contributions to the CMIP5 archive. Journal of Advances in Modeling Earth Systems, 6(1), 141-184.

Shakun, J. D., & Carlson, A. E. (2010). A global perspective on Last Glacial Maximum to Holocene climate change. Quaternary Science Reviews, 29(15-16), 1801-1816.

Shanahan, T. M., McKay, N. P., Hughen, K. A., Overpeck, J. T., Otto-Bliesner, B., Heil, C. W., King, J., Scholz, C. A., & Peck, J. (2015). The time-transgressive termination of the African Humid Period. Nature Geoscience, 8(2), 140-144.

Sime, L. S., Hodgson, D., Bracegirdle, T. J., Allen, C., Perren, B., Roberts, S., & de Boer, A. M. (2016). Sea ice led to poleward-shifted winds at the Last Glacial Maximum: the influence of state dependency on CMIP5 and PMIP3 models. Climate of the Past, 12(12), 2241-2253.

Street, F. A., & Grove, A. T. (1979). Global maps of lake-level fluctuations since 30,000 yr BP. Quaternary Research, 12(1), 83-118.

Street-Perrott, F.A., Marchand, D.S., Roberts, N., & Harisson, S.P. (1989). Global Lake-Level Variations from 18,000 to 0 Years Ago: A Paleoclimatic Analysis. U.S. Department of Energy Technical Report 46, Washington, D.C. 20545. Distributed by National Technical Information Service, Springfield, VA 22161.

Tabor, K., & Williams, J. W. (2010). Globally downscaled climate projections for assessing the conservation impacts of climate change. Ecological Applications, 20(2), 554-565.

Taylor, K. E., Stouffer, R. J., & Meehl, G. A. (2012). An overview of CMIP5 and the experiment design. Bulletin of the American Meteorological Society, 93(4), 485-498.

Tierney, J. E., Smerdon, J. E., Anchukaitis, K. J., & Seager, R. (2013). Multidecadal variability in east african hydroclimate controlled by the indian ocean. Nature, 493(7432), 389-392.

Trenberth, K. E., Dai, A., Schrier, G. V. D., Jones, P. D., Barichivich, J., Briffa, K. R., & Sheffield, J. (2013). Global warming and changes in drought. Nature Climate Change, 4(1), 17-22.

UNEP. (1992). World Atlas of Desertification. Edward Arnold, London.

Voldoire, A., Sanchez-Gomez, E., Salas y Mélia, D., Decharme, B., Cassou, C., Sénési, S., Valcke, S., Beau, I., Alias, A., Chevallier, M., Déqué, M., Deshayes, J., Douville, H., Fernandez, E., Madec, G., Maisonnave, E., Moine, M.-P., Planton, S., Saint-Martin, D., Szopa, S., Tyteca, S., Alkama, R., Belamari, S., Braun, A., Coquart, L., and Chauvin, F. (2013). The CNRM-CM5.1 global climate model: description and basic evaluation. Climate Dynamics, 40(9), 2091-2121.

Wang, G., Garcia, D., Liu, Y., De Jeu, R., & Dolman, A. J. (2012). A three-dimensional gap filling method for large geophysical datasets: Application to global satellite soil moisture observations. Environmental Modelling & Software, 30, 139-142.

Wang, J., Song, C., Reager, J. T., Yao, F., Famiglietti, J. S., Sheng, Y., MacDonald, G. M., Brun, F., Schmied, H. M., Marston, R. A., & Wada, Y. (2018). Recent global decline in endorheic basin water storages. Nature Geoscience, 11(12), 926-932.

Wang, P. X., Wang, B., Cheng, H., Fasullo, J., Guo, Z. T., Kiefer, T., & Liu, Z. Y. (2014). The global monsoon across timescales: coherent variability of regional monsoons. Climate of the Past, 10(6), 2007.

Wang, P. X., Wang, B., Cheng, H., Fasullo, J., Guo, Z., Kiefer, T., & Liu, Z. (2017). The global monsoon across time scales: Mechanisms and outstanding issues. Earth-Science Reviews, 174, 84-121.

Watanabe, S., Hajima, T., Sudo, K., Nagashima, T., Takemura, T., Okajima, H., Nozawa, T., Kawase, H., Abe, M., and Yokohata, T. (2011). MIROC-ESM 2010: Model description and basic results of CMIP5-20c3m experiments. Geoscientific Model Development, 4(4), 845.

Wilby, R. L., Charles, S. P., Zorita, E., Timbal, B., Whetton, P., & Mearns, L. O. (2004). Guidelines for use of climate scenarios developed from statistical downscaling methods.

Wurtsbaugh, W. A., Miller, C., Null, S. E., DeRose, R. J., Wilcock, P., Hahnenberger, M., Howe, F., & Moore, J. (2017). Decline of the world's saline lakes. Nature Geoscience, 10(11), 816-821.

Xi, C., Wang, S., Hu, Z., Zhou, Q., & Qi, H. (2018). Spatiotemporal characteristics of seasonal precipitation and their relationships with enso in central asia during 1901–2013. Journal of Geographical Sciences, 28(9), 1341-1368.

Xue, B., Yu, G., & Zhang, F. J.(2017). Late quaternary lake database in China. Science Press, Beijing, China.

Du, W., Kang, S., Qin, X., Ji, Z., Sun, W., Chen, J., Yang, Y., & Chen, D. (2020). Can summer monsoon moisture invade the Jade Pass in Northwestern China?. Climate Dynamics, 1-15.

Yu, G., Harrison, S. P., & Xue, B. (2001). Lake status records from China: data base documentation. MPI-BGC Tech Rep 4.

Yukimoto, S., Adachi, Y., Hosaka, M., Sakami, T., Yoshimura, H., Hirabara, M., Tanaka, T. Y., Shindo, E., Tsujino, H., and Deushi, M. (2012). A new global climate model of the Meteorological Research Institute: MRI-CGCM3: Model description and basic performance. Journal of the Meteorological Society of Japan, 90, 23-64.

Zhang, J., Chen, F., Holmes, J. A., Li, H., Guo, X., Wang, J., Li, S., Lü, Y., Zhao, Y., & Qiang, M. (2011). Holocene monsoon climate documented by oxygen and carbon isotopes from lake sediments and peat bogs in China: a review and synthesis. Quaternary Science Reviews, 30(15-16), 1973-1987.

Zhan, S., Song, C., Wang, J., Sheng, Y., & Quan, J. (2019). A global assessment of terrestrial evapotranspiration increase due to surface water area change. Earth's future, 7(3), 266-282.

Zhang E, Zhao C, Xue B, Liu, Z., Yu, Z., Chen, R., & Shen, J.. (2017). Millennial-scale hydroclimate variations in southwest China linked to tropical Indian Ocean since the Last Glacial Maximum. Geology, 45(5), 435-438.